Impact of steel slag on the ammonium adsorption by zeolite and a new configuration of zeolite-steel slag substrate for constructed wetlands

Pengbo Shi, Yingbo Jiang, Hongtao Zhu and Dezhi Sun

ABSTRACT

The CaO dissolution from slag, as well as the effects of influencing parameters (i.e. pH and Ca^{2+} concentration) on the ammonium adsorption onto zeolite, was systematically studied in this paper. Modeling results of Ca^{2+} and OH^- release from slag indicated that pseudo-second-order reaction had a better fitness than pseudo-first-order reaction. Changing pH value from 7 to 12 resulted in a drastic reduction of the ammonium adsorption capacity on zeolite, from the peak adsorption capacity at pH 7. High Ca^{2+} concentration in solution also inhibited the adsorption of ammonium onto zeolite. There are two proposed mechanisms for steel slag inhibiting the ammonium adsorption capacity of zeolite. On the one hand, OH^- released from steel slag can react with ammonium ions to produce the molecular form of ammonia ($NH_3{\cdot}H_2O$), which would cause the dissociation of NH_4^+ from zeolite. On the other hand, Ca^{2+} could replace the NH_4^+ ions to adhere onto the surface of zeolite. An innovative substrate filling configuration with zeolite placed upstream of the steel slag was then proposed to eliminate the disadvantageous effects of steel slag. Experimental results showed that this novel filling configuration was superior to two other filling configurations in terms of ammonium removal.

Key words | adsorption, ammonium nitrogen, constructed wetlands, steel slag, substrate filling configuration, zeolite

Pengbo Shi
Yingbo Jiang
Hongtao Zhu (corresponding author)
Dezhi Sun
College of Environmental Science and Engineering,
Beijing Forestry University,
Beijing 100083,
China
E-mail: *zhuhongtao@bjfu.edu.cn*

Pengbo Shi
State Grid Beijing Electric Power Research Institute,
Beijing 100075,
China

INTRODUCTION

Nitrogen and phosphorus are essential nutrients for biomass growth. But excessive nitrogen and phosphorus can contribute to accelerated eutrophication of lakes and rivers. The eutrophication causes a rapid growth of algae and other microorganisms, resulting in dissolved oxygen depletion and fish toxicity. The removal of nitrogen and phosphorus has not recently become an important and urgent wastewater treatment task but has, in fact, been studied for a long time now.

Constructed wetlands are an efficient and eco-friendly form of wastewater treatment technology with low operating cost and low-energy consumption. This technology has been widely used to relieve the eutrophication of waters and restore ecosystems for dozens of years (Tanner *et al.* 2002; Bezbaruah & Zhang 2003; Mateus *et al.* 2012). As one of the most important parts of constructed wetlands, the substrate can partly determine the removal or form-converting efficiency of nitrogen and phosphorous. Thus, to increase the nutrient removal efficiency of constructed wetlands, substrates should be selected and grouped carefully.

Because of high affinity with ammonium ion, zeolite, as a common substrate, is applied in constructed wetlands worldwide. Many studies have confirmed that zeolite has a good performance of nitrogen removal (Du *et al.* 2005; Alias *et al.* 2010; Huang *et al.* 2010; Beebe *et al.* 2013). Ion-exchange is considered to be a significant mechanism for adsorption of ammonium ion onto zeolite (Wang *et al.* 2007). In constructed wetland, ammonium ion could be adsorbed by zeolite via ion exchange, and then under proper conditions oxidized to nitrite first and then nitrate. Nitrogen can be removed from water in a biological denitrification process when nitrate and electron donor (i.e. chemical oxygen demand, COD) are present. The adsorption of ammonium ion by zeolite might be a step for nitrogen removal enhancement (Beebe *et al.* 2013).

Another substrate seen commonly for constructed wetlands is steel slag, which is the molten byproduct of many

doi: 10.2166/wst.2017.232

metallurgical operations. It has high contents of Ca, Al, or Fe, and possesses a strong affinity with phosphate (i.e. PO_4^+-P) (Kostura *et al.* 2005; Johansson-Westholm 2006; Chris *et al.* 2007). Several authors have confirmed that steel slag is a better substrate for phosphorus removal compared to soil, zeolites, and so on (Mann 1997; Brix *et al.* 2001). The major PO_4^+-P removal mechanism is precipitation of Ca-PO_4-P complexes with the release of Ca^{2+} from steel slag (Drizo *et al.* 2002, 2006; Barca *et al.* 2012, 2014; Claveau-Mallet *et al.* 2013). Iron-phosphate formation was also confirmed as another way for phosphorus removal (Pratt *et al.* 2007). Claveau-Mallet *et al.* (2014) have modeled the dissolution and precipitation of phosphorus removal by slag filter.

Due to the excellent ammonium removal ability of zeolite and phosphate removal ability of steel slag, they have been combined in the substrate bed of a constructed wetland in order to enhance the simultaneous removal efficiencies of nitrogen and phosphorus. Actually, in the study of Olfa *et al.* (2002), a porous carrier made from artificial zeolite and acidic treated blast furnace slag had better removal efficiency for phosphate and ammonium.

In our early tests, zeolite and steel slag were combined with each other in order to simultaneously achieve a high removal efficiency of ammonium-nitrogen and phosphate-phosphorus. However, compared with the results when only zeolite was used, the removal efficiency of ammonia was sharply decreased when zeolite and steel slag were used together. No similar reports were made in studies of this field as a reason of differently treated substrates being used (e.g. Olfa *et al.* 2002; Renman *et al.* 2009; Lee *et al.* 2010). Until now, the mechanism of steel slag affecting the adsorption of ammonium onto zeolite still lacks a systematic study.

The objective of this paper was to explore the interaction mechanism behind steel slag and zeolite when targeting the removal of ammonium. Based on the interaction mechanism, a new substrate bed configuration was going to be proposed to eliminate the disadvantageous effects of steel slag, and to simultaneously achieve higher removal efficiencies for nitrogen and phosphorus.

METHODS

Substrates collection and preparation

Zeolite and steel slag were selected as substrate subjects in this study according to their NH_4^+-N and PO_4^+-P removal ability obtained in pre-study tests. In the pre-study tests, zeolite showed best NH_4^+-N removal ability and steel slag showed best P removal ability among all eight types of substrates including shale, ceramisites made of various materials, steel slag and zeolite. Zeolite was obtained from KaiBiYuan Trading Co. Ltd (Beijing, China), and steel slag was supplied by a steel plant in Jiangxi Province. To prepare similarly sized substrate particles for tests, the samples were first screened on an automatic grinder according to three ranges of granular sizes (i.e. <2, 2–5 and >5 mm). The granular size of 2–5 mm was then selected to perform the batch experiments. This guarantees the results to be comparable. Before used in tests, substrates were rinsed with tap water to remove impurities and fine particles attached to their surface. The clean substrates were dried at 105 °C for 24 h. Energy dispersive spectrometer X-ray (EDS, 7021-H, Horiba, Japan) was performed to quantify the elemental composition on substrate surfaces.

Kinetic experiments on Ca^{2+} and OH^- release from steel slag

Two series of batch experiments were carried out to verify the kinetics of Ca^{2+} and OH^- release from slag. Batch experiments were to verify if the increase of Ca^{2+} and pH of the solutions depended primarily on CaO-slag dissolution. Forty grams of slag were added into triangular flasks, which contained 1 L of deionized water (conductivity <30 μS/cm) and 25 mg/L ammonium nitrogen solution, separately. Two drops of chloroform were dosed into the prepared solutions for the inhibition of microorganisms' growth. The flasks were then placed on an agitation table and shaken at 150 rpm under the controlled temperature condition of 25 °C for 4 days. During 4 days agitation, samples were taken at the end of the 2nd, 4th, 8th, 12th, 24th, 36th, 48th, 72th, and 96th hour for pH and Ca^{2+} concentrations measurements. The pH of the solutions could be expressed in OH^- concentration. Equations (1) and (2) were used in this study to calculate the experimental capacities of Ca^{2+} and OH^- released from steel slag.

$$Q_t = \frac{Ca_t V}{M} \tag{1}$$

$$Q_t = \frac{OH_t V}{M} \tag{2}$$

where Q_t (mg/g) are the capacities of Ca^{2+} and OH^- release at time t (h), V (L) is the volume of the solution, M (g) is the

mass of steel slag, Ca_t and OH_t (mg/L) are the Ca^{2+} and OH^- concentration of the solutions at time t (h).

Influence of Ca^{2+} and OH^- on ammonium adsorption onto zeolite

In order to examine the various effects of Ca^{2+} and OH^- on ammonium adsorption performance, two series of tests were conducted. For each series of tests, 20 g of zeolite was immersed in 500 mL 25 mg N/L ammonium solution contained in triangular flasks, thus leading to a zeolite to solution ratio of 0.04 g per mL. For OH^- tests, the initial pH values in flasks were adjusted to 4, 5, 6, 7, 8, 9, 10, 11, and 12 with 0.5 mol/L HCl and 0.1 mol/L NaOH. For Ca^{2+} tests, the concentration of Ca^{2+} was prepared at 0, 5, 10, 20, 40, 60, 80, 120, 140, 180 mg/L, respectively. Two drops of chloroform were also dosed for the inhibition of microorganism in each flask. The flasks were then placed on agitation tables and shaken at 150 rpm under controlled temperature conditions (25 °C) for 4 days.

Influence of steel slag on zeolite saturated with ammonium

To prepare zeolite saturated with ammonium, 40 g of zeolites was immersed in 1 L of 25 mg/L ammonium solution, and then was shaken at 150 rpm under 25 °C for 4 days under sterilized circumstances. Forty grams of steel slag was added into the flask with ammonium-saturated zeolite for another 4 days' agitation. During the second 4 days' agitation, solution samples were taken at a serial hours for pH, ammonium nitrogen and Ca^{2+} measurements.

Optimization of the substrate bed configuration

Three identical cylinders with the height and diameter 40 × 6 cm were used as laboratory-scale reactors (marked as A, B, and C, respectively). Each cylinder was filled with exactly the same quantity of zeolite and steel slag by using different configurations (Table 1). The placing order of substrates in reactor A was that, 10 cm of steel slags first and then 20 cm of zeolites from the bottom up. The B reactor was filled with 30 cm mixture of zeolites and steel slags. For reactor C, the sequence was opposite to reactor A. Figure 1 shows the schematic diagram of all three reactors. In all three tests, synthetic wastewater was used as influent, which was pumped into reactors from the bottom inlet. Main parameters of the synthetic wastewater was listed as pH 6.8–7.4, NH_4^+-N 25 mg·L^{-1}, PO_4^{3-} 5 mg·L^{-1}. The inflow rate was set at 0.15 mL·min^{-1}. Both effluent and influent samples were taken from the three reactors every other day for pH, NH_4^+-N and PO_4^{3-} measurements. The cylinders were operated for 2 months running.

Table 1 | Substrate configuration in reactor A through C

Reactor	Description
A	From bottom up: 10 cm steel slag; 20 cm zeolite
B	30 cm mixture of zeolites and steel slags, volumetric ratio 2:1
C	From bottom up: 20 cm zeolite; 10 cm steel slag

Analytical methods

Phosphate, NH_4^+-N and Ca^{2+} analyses were performed according to the Ammonium Molybdate Spectrometric Method, Nessler's reagent Spectrometric Method and the Atomic Absorption Spectrometric Method, respectively. Phosphate and NH_4^+-N concentrations were measured using a MI-parameter Meter (5B-3B, LianHua, China), whereas Ca^{2+} concentrations were measured using an Atomic Absorption Spectrophotometer (AA6300, Shimadzu, Japan). The pH value was measured with a pH meter (WTW, Germany).

RESULTS AND DISCUSSION

Chemical composition of substrates

The chemical composition of substrates plays an important role in their pollutant removal ability. The results of EDS

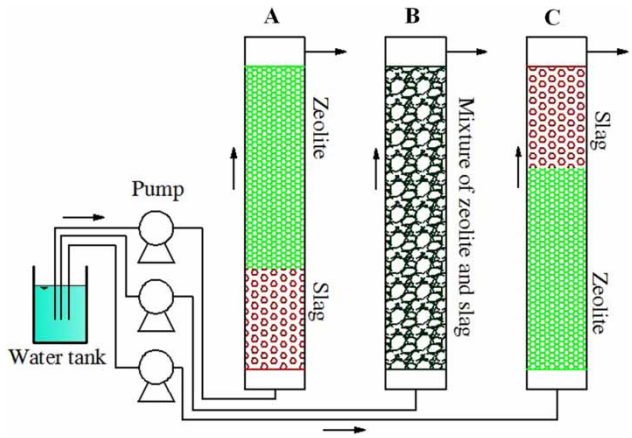

Figure 1 | The schematic diagram of all three reactors.

analyses (shown in Table 2) show the main chemical composition of the surfaces of zeolite and steel slag. Based on Table 2, aluminosilicate minerals dominate the surface of zeolite, which are mainly composed of silicon, oxygen and aluminum. According to other related reports (Alias *et al.* 2010; Huang *et al.* 2010), the structure of zeolite is networks of tetrahedral or polyhedral arrangements of atoms, as well as microporous, which works as an mechanical sieve. These structures decide that zeolite has a better adsorption capacity for ammonium. Steel slag is rich in CaO. These results are in agreement with findings of other reported studies on slag composition (Drizo *et al.* 2002; Xue *et al.* 2009; Wang *et al.* 2010; Barca *et al.* 2012).

Kinetics of Ca^{2+} and OH^- release from steel slag

To elucidate the kinetics of Ca^{2+} and OH^- release from steel slag, and the interrelationship between steel slag and ammonium solution, two series of batch experiments were conducted, the methods of which were described in the Methods section above. The experimental results showed that Ca^{2+} concentrations and pH values of the solutions changed with soaking time (shown in Figure 2). It can be seen from Figure 2 that, no matter whether in deionized water or in ammonium solution, Ca^{2+} concentrations and pH values of the solutions increased quickly until a (pseudo-) equilibrium was reached at some time between the 36th and 48th hour of agitation and had small variations after then. These curves can be explained by following CaO-slag dissolution Equation (3). Several authors have also confirmed that steel slag had a particularly strong tendency to produce basic leachates as a result of a mixture of dissolution reactions of various metal oxides, including CaO, Al_2O_3, and MgO (Bowden *et al.* 2009; Xue *et al.* 2009).

$$CaO + H_2O \longrightarrow Ca^{2+} + 2OH^- \quad (3)$$

Table 2 | EDS analyses: chemical composition of zeolite and steel slag (weight %)

	Zeolite	Steel slag
SiO_2(%)	51.54–60.13	0.60–1.52
Fe_2O_3(%)	2.03–4.73	–
Al_2O_3(%)	9.39–10.50	–
CaO(%)	2.42–3.44	35.98–37.59
MgO(%)	0.47–0.93	0.32–0.52
C(%)	2.78–3.01	9.12–9.77
N(%)	5.01–5.56	8.88–9.02

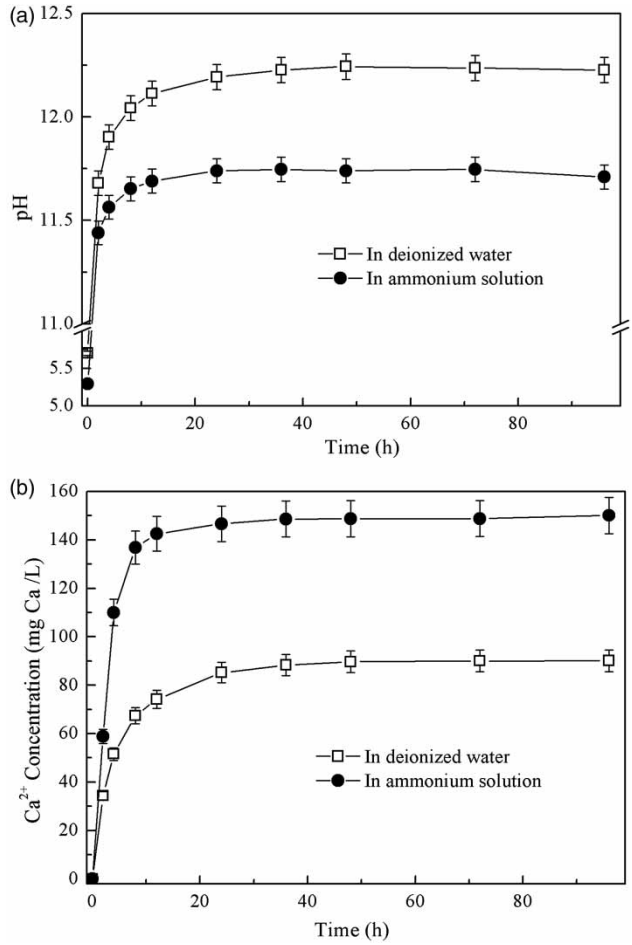

Figure 2 | Variation of Ca^{2+} and OH^- concentration with time in different original solutions: pH (a) and Ca^{2+} concentration (b).

Obviously, the existence of ammonium ions influenced the CaO dissolution from steel slag. From Figure 2(a), it can be seen that pH value in deionized water was higher than that in ammonium solution. However, the situation was opposite for Ca^{2+}. From Figure 2(b), the Ca^{2+} release capacity of steel slag in ammonia solution was higher than in deionized water. Equation (4), which describes ammonia dissociation in water, may explain the phenomenon that the variation of Ca^{2+} concentration differed with that of OH^- concentration. In ammonia solution, the OH- produced by CaO dissolution was consumed by ammonium ion via transformation to molecular form ammonia ($NH_3{\cdot}H_2O$) (see Equation (4)). Therefore, the pH curve of ammonia solution lies below its counterpart of deionized water. At the same time, the consumption of OH^- leads to further dissociation of CaO-slag (Equation (3)). As a result, it can be explained why Ca^{2+} curve of steel slag in ammonia solution was above that in deionized water. As shown in Table 2, no

matter in deionized water or in ammonium solution, the equilibrium capacities Q_e and the rate constants k_2 of Ca^{2+} and OH^- release do not agree with each other. This could be attributed to the influence of ammonia on Equation (3) as stated in paragraph above.

$$NH_4^+ + OH^- \longleftrightarrow NH_3 \bullet H_2O \quad (4)$$

The kinetics of CaO-slag dissolution has been modeled by Barca *et al.* (2012), and in their study, high correlation coefficients were obtained when a pseudo-first-order kinetic model was used for European steel slag. Thus, in this study, the kinetics of Ca^{2+} and OH^- release was first modeled based upon experimental results in Figure 2 with the pseudo-first-order kinetic reaction (see Equation (5)). However, the fitting results ($R^2 < 0.9$) were not as good as expected. Then the pseudo-second-order kinetic reaction (Equation (6)) was employed for further modeling.

The pseudo-first-order kinetic equation:

$$\ln(Q_e - Q_t) = \ln Q_e - k_1 t \quad (5)$$

The pseudo-second-order equation:

$$\frac{t}{Q_t} = \frac{1}{k_2 Q_e^2} + \frac{t}{Q_e} \quad (6)$$

where k_1 (h^{-1}) and k_2 ($g \cdot mg^{-1}\, h^{-1}$) are constants of release rate, Q_t ($mg \cdot g^{-1}$) is the release capacity at time t (h), Q_e ($mg \cdot g^{-1}$) is the release capacity at equilibrium (Ho & McKay 1999).

The modeling results of Ca^{2+} and OH^- release from slag indicated that pseudo-second-order reaction had a better fitness (much higher R^2 shown in Table 3). Barca *et al.* (2012) reported that CaO was present in great excess over the other reactants in the reaction mixture, and the dissolution of CaO-slag was the primary reaction explaining the increase of Ca^{2+} and pH in solution. However, in this study, the lower applicability of the pseudo-first-order model to describe Ca^{2+} release ($R^2 < 0.9$, data not shown) gave another different picture for the dissolution of CaO-slag.

Table 3 | Correlation coefficients and rate constants for the pseudo-second-order kinetic model describing Ca^{2+} and OH^- release

	Ca^{2+} release			OH^- release		
Steel slag	Q_e (mg Ca/g)	k_2 (g/mg h)	R^2	Q_e (mg OH/g)	k_2 (g/mg h)	R^2
In deionized water	2.41	92.01	0.998	8.18	3.90	0.997
In 25 mg/L ammonia	4.28	6.64	0.925	2.43	22.88	0.987

Weathering has an influence on steel slag changing the Ca^{2+} and OH^- release capacity (Wang *et al.* 2010; Barca *et al.* 2012). This might have affected the steel slag used within this study as it was exposed to weathering over an uncertain period of time before being used in the experiments. During the weathering of steel slag, a certain amount of $Ca(OH)_2$ and $CaCO_3$ might be converted from CaO. The dissolution of CaO-slag in this study might contain three parts: (1) the dissolution of CaO-slag, (2) the dissolution of $Ca(OH)_2$-slag, and (3) the constraint from $CaCO_3$ covered on the surface of steel slag. The dissolution of $Ca(OH)_2$ is probably different from CaO. $CaCO_3$ is not dissolved in water, therefore, it would act like a cover to inhibit the dissolution of CaO or $Ca(OH)_2$.

The influence of Ca^{2+} and OH^- on the adsorptive performance of ammonia nitrogen onto zeolite

Two series of tests were conducted to examine the various effects of Ca^{2+} and OH^- concentrations on ammonia nitrogen adsorption performance. The experimental results are shown in Figure 3. In one of the series (shown in Figure 3(a)), initial pH ranges were set from 4 to 12. It can be seen from that the adsorption capacity of ammonium ion increased slightly with the pH changed from 4 to 7. When pH value of the solution was 7, the adsorption capacity of ammonium ion reached a peak. Moreover, pH changing from 7 to 12 resulted in a drastic reduction of the ammonium ion adsorption capacity. The experimental results indicated that the adsorption capacity for ammonium onto zeolite was obviously impacted by pH of ammonium solution. This phenomenon was also widely reported by other authors (e.g. Du *et al.* 2005; Beebe *et al.* 2013). The reason might be that pH can influence both the character of the exchanging ions and the character of zeolite itself.

In solutions at pH below 7, ammonium ion is the dominant specie of ammonium chloride solution. As a competitor for exchanging sites on zeolite with ammonium ions, the number of H^+ ion also rises at low pH, which explains the slight increase in adsorption capacity of ammonium ion from pH 4 to 12. At pH above 7, the reduction of NH_4^+ adsorption capacity can be understandable by considering the transformation among NH_4^+ and $NH_3 \cdot H_2O$ with pH changing (see Equation (4)). Certainly, when the molecular form ammonia (NH_3) is dominant in solution at high pH, the ion exchanging adsorption onto

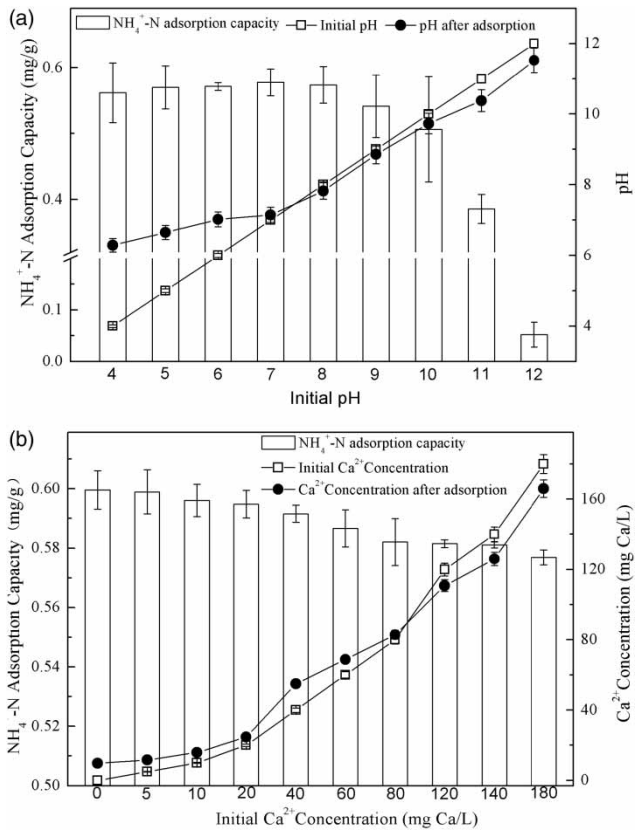

Figure 3 | Effects of initial solution conditions on the NH_4^+ adsorption performance of zeolite: (a) pH; and (b) Ca^{2+} concentration.

zeolite would be damaged badly. On the other hand, Lee *et al.* (2010) and Renman *et al.* (2009) have stated that elevated pH (>10) caused by steel slag filter could shift the activity of ammonium species towards unionized ammonia (pKa for ammonium is 9.24, and above this value, NH_3 is the predominant form), which might be more readily volatilized. This might be another reason for the reduction of NH_4^+ adsorption capacity at pH > 7.

Compared with the initial solutions at pH below 7, the pH value rose after adsorption equilibrium (see Figure 3(a)). This is probably because parts of H^+ ions were adsorbed. For solutions at pH above 9, the reduction of pH after adsorption processes is due to part of molecular-formed ammonia transforming into ammonia gas.

The concentration of Ca^{2+} also has a great impact on the adsorption capacity of ammonium ions onto zeolite. As observed in Figure 3(b), the adsorption capacity of ammonium onto zeolite decreased gradually with the increase of Ca^{2+} concentration. It indicates that high Ca^{2+} concentration in solution can inhibit the adsorption of ammonium onto zeolite. In general, the ion exchange preferential order goes as following: $K^+ > NH_4^+ > Na^+ > Ca^{2+} > Fe^{3+} > Al^{3+} > Mg^{2+}$ (Tsitsis & Ronikashvili. 1992). At lower Ca^{2+} concentration, ammonium ion is adsorbed by zeolite in preference to calcium ion. Therefore, calcium ions, which are already adsorbed onto zeolite, might be replaced by ammonium ions. However, at higher Ca^{2+} concentration, the ammonium ions have to compete with calcium ions for being adsorbed onto exchange sites as the Ca^{2+} concentration increases. Equilibrium between the two species would be reached at last. As a result, adsorption of calcium ions onto zeolite caused the reduction of adsorption capacity of ammonium ion. This theory could also be confirmed by comparing Ca^{2+} concentrations before and after adsorption experiments, which shows that (1) the Ca^{2+} concentration after adsorption was greater than the corresponding initial values when that initial values were below 80 mg Ca/L and (2) the Ca^{2+} concentration after adsorption was lower than the corresponding initial values when that initial values were above 80 mg Ca^{2+} per liter. Under the condition of 20 g zeolite in 500 mL aqueous solution, the equilibrium concentrations for Ca^{2+} and NH_4^+ are 80 $mg \cdot L^{-1}$ and 0.8 $mg \cdot L^{-1}$, respectively.

The influence of steel slag on zeolite saturated with NH_4^+-N

In order to simulate the situation of steel slag being placed ahead of zeolite, two tests were carried out to further explore the inhibition mechanism of steel slag on NH_4^+ adsorption onto zeolite. In one test, steel slag was added into aqueous solution with NH_4^+ saturated zeolite. In another contrast test, there was only zeolite saturated with NH_4^+ in solution. Pseudo-equilibrium of zeolite adsorbing NH_4^+-N was assumed being achieved after 4 days of agitation. After equilibrium, steel slag was added in. The variation of pH, Ca^{2+} and NH_4^+-N concentrations in both tests are illustrated in Figure 4. For the control sample (without steel slag), pH, Ca^{2+} and NH_4^+-N concentrations of the solution had no large fluctuation from the 96th hour on. But in another test (where steel slag was added), the pH and Ca^{2+} concentration skyrocketed to a high level in 4 to 8 h after the steel slag addition (steel slag was added at the 96th hour). Whereafter, both pH and Ca^{2+} concentration decreased gradually and slightly from the 104th hour to the end of the tests. The NH_4^+-N concentration increased after the addition of steel slag, and the final value was close to the initial NH_4^+-N concentration. The NH_4^+-N release was probably because of the change of pH and Ca^{2+} concentrations in solution. Equations (7) and (8) can

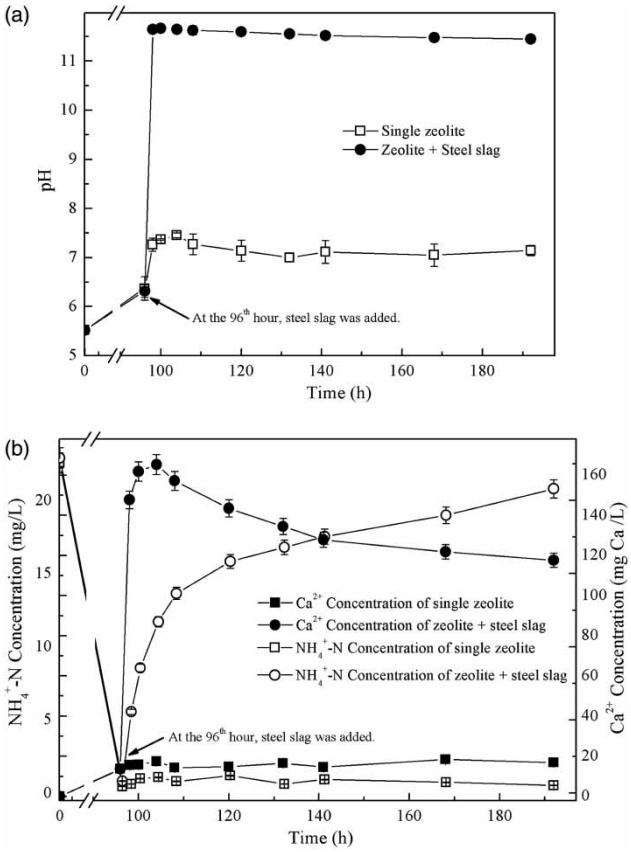

Figure 4 | The influence of steel slag on zeolite saturated with NH_4^+: (a) pH; (b) Ca^{2+} and NH_4^+.

be used to calculate the correlation parameter.

$$2NH_{4(Z)}^{+} + Ca_{(S)}^{2+} + 2OH_{(S)}^{-} \longleftrightarrow Ca_{(Z)}^{2+} + NH_3 \bullet H_2O_{(S)} \quad (7)$$

$$NH_3 \bullet H_2O_{(S)} \longrightarrow NH_{3(G)} \uparrow + H_2O_{(S)} \quad (8)$$

$$N = \frac{(C_{max} - C_{min})V}{M} \quad (9)$$

The subscripts Z, S and G refer to on zeolite, in aqueous solution and in gas phase, respectively. Where N (mol) is molar mass, C_{max} (mg/L) are the maximum values of the Ca^{2+}, OH^- and NH_4^+-N concentrations, C_{min} are minimum values of the Ca^{2+}, OH^- and NH_4^+-N concentrations, V (L) is the volume of the solution, M is relative molecular mass.

According to Equation (7), the released capacity of NH_4^+-N should be equal to the reduced capacity of OH^- or to two folds of reduced capacity of Ca^{2+}, respectively. The maximum and minimum values of pH, Ca^{2+} and NH_4^+-N concentrations were then selected to calculate their amount of substance according to Equation (9). The values of C_{max}, C_{min} and N (i.e. the amount of substance) of Ca^{2+}, OH^- and NH_4^+-N are shown in Table 4. Due to molecular form ammonia being a volatile liquid, a portion of ammonia ($NH_3.H_2O$) was expected to transform into ammonia gas (NH_3), which would volatilize into atmosphere and do not determine NH_4^+-N concentration in solution. Thus, it can be confirmed that the reduced capacity of OH^- is approximately equal to the released capacity of NH_4^+-N (1.43 mmol NH_4^+-N + volatile ammonia gas (NH_3) ≈ 1.73 mmol OH^-). But, the reduced capacity of Ca^{2+} was much more than expected, i.e. a half of the released capacity of NH_4^+-N (1.35 mmol Ca^{2+} > 0.5*1.43 mmol NH_4^+-N). The unaccounted-for reduced capacity of Ca^{2+}, i.e. approximately 0.63 mmol, probably adhered onto the surface of zeolite in forms of solid crystal or cation. And the proof based upon scanning electron microscopy (SEM) morphological analysis of zeolite surface would be stated in the next sector. It can be told that the surface of zeolite in zeolite-steel group was covered by crystal substance. Based upon this evidence, a deduction can be made that steel slag inhibits the ammonium adsorption capacity of zeolite, mainly because of the release of Ca^{2+} and OH- from steel slag. Ammonium ions can react with hydroxyl ion to produce molecular form ammonia ($NH_3 \cdot H_2O$), which would cause the dissociation of NH_4^+ from zeolite. Whereafter, a quantity of Ca^{2+} will replace the NH_4^+ ions to adhere onto the surface of zeolite. Thus, the existence of steel slag would result in a poor adsorption capacity of ammonium ion onto zeolite.

Optimization of the substrates bed configuration

Based on the inhibition effects of steel slag on zeolite adsorbing NH_4^+-N, a new substrate bed configuration that zeolites are placed upstream, followed by steel slag downstream, was proposed to eliminate the disadvantageous effect of steel slag. Zeolite and steel slag were filled into reactor C according to this bed configuration. At the same time, as a contrast, two other bed configurations are also prepared (sequentially there was steel slag and zeolite in reactor A

Table 4 | Values of C_{max}, C_{min} and N (i.e. the amount of substance) of Ca^{2+}, OH^- and NH_4^+-N

	OH^-	NH_4^+-N (as N)	Ca^{2+}
C_{max} (mg/L)	77.69	20.81	165.26
C_{min} (mg/L)	48.25	0.83	117.65
N (mmol)	1.73	1.43	1.19

from the bottom up, and in reactor B zeolite and steel slag were all mixed up). During the period of operation, three reactors all showed relatively stable and high efficiency for phosphate removal, exhibiting the configuration of zeolite and steel slag having no effect on the phosphate removal. The P removal rate ranges for A, B, and C were all in the range of 80–90%.

However, it can be seen from Figure 5 that different bed configurations of zeolite and steel slag have significant effects on NH_4^+-N removal. The average removal efficiency of reactor C is obviously higher than reactors A and B. This result has a good agreement with our expectation. In reactor C, the wastewater flowed through zeolite layer and steel slag layer sequentially. Zeolite layer can provide substantial removal of nitrogen from wastewater. In this progress, the Ca^{2+} and OH^- of steel slag had not yet released into wastewater. When wastewater flowed through the steel slag layer, the released Ca^{2+} and OH^- outflowed from the top of reactor with wastewater, and could not affect the adsorption of ammonium ion on zeolite.

The NH_4^+-N concentration in the effluent of reactor A kept rising from the 23th day (as shown in Figure 5).

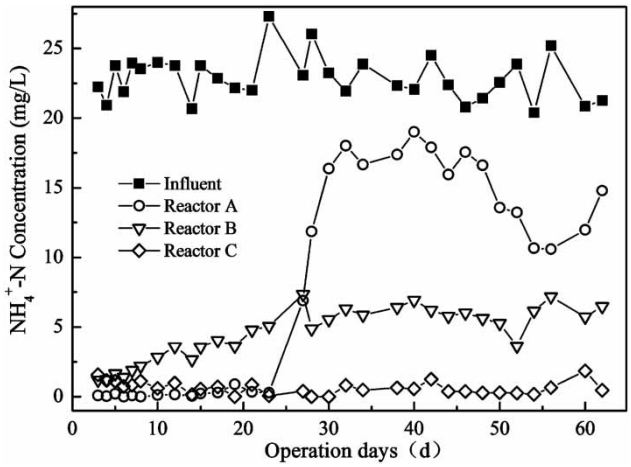

Figure 5 | Optimization of three substrates bed configurations.

Figure 6(c) shows the SEM pictures of zeolite particles sampled from the bottom of zeolite layer before the 23th day. Crystal substance can be seen on the surface of zeolite particles. While, at the same time, this crystal substance could not be found on zeolite particles in reactor C, as well as on zeolite particles sampled from the top of zeolite layer in reactor A. The chemical composition of the crystals is calcium and oxygen based upon the results of EDS. Obviously, calcium crystal is prone to adhere onto the surface of zeolite particles immediately when they encounter each other. Therefore, as the operation goes on, more and more zeolite particles from the bottom up were covered by the crystal, and lost their ammonia nitrogen adsorption ability. Zeolite could be viewed as a 'buffer' to decrease the bad impact of high Ca^{2+} and OH^- concentrations. In reactor A, this buffer capacity of zeolite decreased gradually and disappeared at the 23rd day from reactor initiating. That explains the phenomenon that, NH_4^+-N removal efficiency declined rapidly from the 23th day in Figure 5. The NH_4^+-N removal efficiency of reactor B was always lower than that in reactor C, and also lower than that in reactor A before the 23th day. The reason might be due to the mixture of two substrates enabling the inhibition effect of steel slag from the very beginning.

CONCLUSIONS

In this study, the relationship and interaction when using steel slag and zeolite in combination on ammonium ions removal has been studied. As steel slag is rich in CaO, the dissolution of CaO off slag happens no matter in water or in NH_4^+ solution, and it results in quick increase of pH and Ca^{2+} concentration in any solutions. An equilibrium was reached at some time between the 36th and 48th hour of agitation and modeling results of Ca^{2+} and OH^- release from slag indicated that pseudo-second-order reaction had a better fitness than pseudo-first-order reaction. The

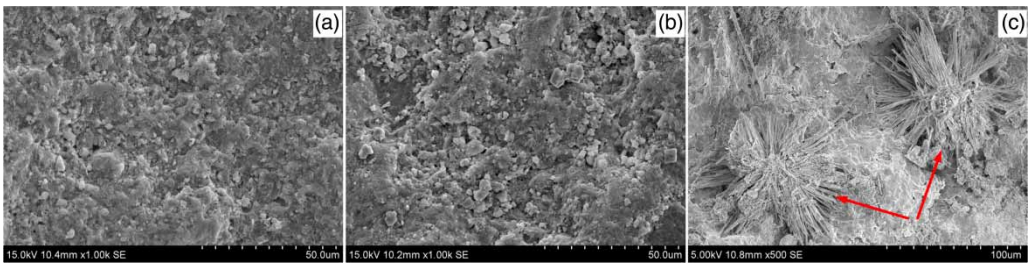

Figure 6 | SEM pictures of zeolite in: (a) column without steel slag; (b) column with steel slag; (c) bottom of zeolite of Reactor A.

existence of NH_4^+ ions influenced the CaO dissolution of steel slag via reacting with OH^-.

Both of pH and Ca^{2+} can change the adsorption capacity of ammonium ion onto zeolite. The pH value changing from 7 to 12 resulted in a drastic reduction of the ammonium ion adsorption capacity from the peak at pH7. The adsorption capacity of ammonium onto zeolite decreased gradually with the increase of Ca^{2+} concentration, indicating that high Ca^{2+} concentration in solution can inhibit the adsorption of ammonium onto zeolite.

The mechanism for steel slag inhibiting the ammonium adsorption capacity of zeolite is that, OH^- released from steel slag can react with ammonium ions to produce molecular form ammonia ($NH_3{\cdot}H_2O$), which would cause the dissociation of NH_4^+ from zeolite. And also, a quantity of Ca^{2+} could replace the NH_4^+ ions to adhere onto the surface of zeolite.

A new substrate bed configuration of zeolites placed upstream, followed by steel slag downstream was proposed to eliminate the disadvantageous effect of steel slag. And experimental results showed that the new bed configuration was superior to the other two contrast patterns in terms of ammonium removal.

ACKNOWLEDGEMENT

This research was supported by the Fundamental Research Funds for the Central Universities (No. 2016ZCQ03).

REFERENCES

Alias, M. Y., Lee, K. K., Zaharah, I., Zaiton, A. M. & Nik, A. N. 2010 Kinetic and equilibrium studies of the removal of ammonium ions from aqueous solution by rice husk ash-synthesized zeolite Y and powdered and granulated forms of mordenite. *Journal of Hazardous Materials* **174** (1–3), 380–385.

Barca, C., Gérente, C., Meyer, D., Chazarenc, F. & Andrès, Y. 2012 Phosphate removal from synthetic and real wastewater using steel slags produced in Europe. *Water Research* **46** (7), 2376–2384.

Barca, C., Meyer, D., Liir, M., Drissen, P., Comeau, Y., Andrès, Y. & Chazarenc, F. 2014 Steel slag filters to upgrade phosphorus removal in small wastewater treatment plants: removal mechanisms and performance. *Ecology Engineering* **68**, 214–222.

Beebe, D. A., Castle James, W. & Rodgers Jr., J. H. 2013 Treatment of ammonia in pilot-scale constructed wetland systems with clinoptilolite. *Journal of Environmental Chemical Engineering* **1** (4), 1159–1165.

Bezbaruah, A. N. & Zhang, T. C. 2003 Performance of a constructed wetland with a sulfur/limestone denitrification section for wastewater nitrogen removal. *Environmental Science & Technology* **37** (8), 1690–1697.

Bowden, L. I., Jarvis, A. P., Younger, P. L. & Johnson, K. L. 2009 Phosphorus removal from waste waters using basic oxygen steel slag. *Environmental Science & Technology* **43** (7), 2476–2481.

Brix, H., Arias, C. A. & Bubba, M. D. 2001 Media selection for sustainable phosphorus removal in subsurface flow constructed wetlands. *Water Science and Technology* **44** (11–12), 47–54.

Chris, P., Andy, S., Steven, P., Richard, G. & Nanthi, S. B. 2007 Phosphorus removal mechanisms in active slag filters treating waste stabilization pond effluent. *Environmental Science & Technology* **41** (9), 3296–3301.

Claveau-Mallet, D., Wallace, S. & Comeau, Y. 2013 Removal of phosphorus, fluoride and metals from a gypsum mining leachate using steel slag filters. *Water Research* **47** (4), 1512–1520.

Claveau-Mallet, D., Courcelles, B. & Comeau, Y. 2014 Phosphorus removal by steel slag filters: modeling dissolution and precipitation kinetics to predict longevity. *Environmental Science & Technology* **48** (13), 7486–7493.

Drizo, A., Comeau, Y., Forget, C. & Chapuis, R. P. 2002 Phosphorus saturation potential: a parameter for estimating the longevity of constructed wetland systems. *Environmental Science & Technology* **36** (21), 4642–4648.

Drizo, A., Forget, C., Chapuis, R. P. & Comeau, Y. 2006 Phosphorus removal by electric arc furnace steel slag and serpentinite. *Water Research* **40** (8), 1547–1554.

Du, Q., Liu, S. J., Cao, Z. H. & Wang, Y. Q. 2005 Ammonia removal from aqueous solution using natural Chinese clinoptilolite. *Separation and Purification Technology* **44** (3), 229–234.

Ho, Y. S. & McKay, G. 1999 Pseudo-second-order model for sorption processes. *Process Biochemistry* **34** (5), 451–465.

Huang, H. M., Xiao, X. M., Yan, B. & Yang, L. P. 2010 Ammonium removal from aqueous solutions by using natural Chinese (Chende) zeolite as adsorbent. *Journal of Hazardous Materials* **175** (1–3), 247–252.

Johansson-Westholm, L. 2006 Substrates for phosphorus removal-potential benefits for on-site wastewater treatment? *Water Research* **40** (1), 23–36.

Kostura, B., Kulveitová, H. & Leško, J. 2005 Blast furnace slags as sorbents of phosphate from water solutions. *Water Research* **39** (9), 1795–1802.

Lee, M. S., Drizo, A., Rizzo, D. M., Druschel, G., Hayden, N. & Twohig, E. 2010 Evaluating the efficiency and temporal variation of pilot-scale constructed wetlands and steel slag phosphorus removing filters for treating dairy wastewater. *Water Research* **44** (14), 4077–4086.

Mann, R. A. 1997 Phosphorus adsorption and desorption characteristics of constructed wetland gravels and steelworks by-products. *Australian Journal of Soil Research* **35** (2), 375–384.

Mateus, D. M. R., Vaz, M. M. N. & Pinho, H. J. O. 2012 Fragmented limestone wastes as a constructed wetland substrate for phosphorus removal. *Ecology Engineering* **41**, 65–69.

Olfa, K., Yasunori, K., Hitoshi, M., Kengo, K. & Mamuro, N. 2002 Nutrients adsorption from seawater by new porous carrier made from zeolitized fly ash and slag. *Marine Pollution Bulletin* **45** (1–12), 311–315.

Pratt, C., Shilton, A., Pratt, S., Haverkamp, R. G. & Bolan, N. S. 2007 Phosphorus removal mechanisms in active slag filters treating waste stabilization pond effluent. *Environmental Science & Technology* **41** (9), 3296–3301.

Renman, A., Hylander, L. G. & Renman, G. 2009 Transformation and removal of nitrogen in reactive bed filter materials designed for on-site wastewater treatment. *Ecology Engineering* **34** (3), 207–214.

Tanner, C. C., Kadlec, R. H., Gibbs, M. M., Sukias, J. P. S. & Nguyen, M. L. 2002 Nitrogen processing gradients in subsurface flow treatment wetlands – Influence of wastewater characteristics. *Ecology Engineering* **18** (4), 499–520.

Tsitsis, H. G. V. & Ronikashvili, T. G. 1992 *Natural Zeolites Chichester*. Ellis Horwood Limited, Hertfordshire, UK.

Wang, Y., Kmiya, Y. & Okuhara, T. 2007 Removal of low-concentration ammonia in water by ion-exchange using Na-mordenite. *Water Research* **41** (2), 269–276.

Wang, G., Wang, Y. H. & Gao, Z. L. 2010 Use of steel slag as a granular material: volume expansion prediction and usability criteria. *Journal of Hazardous Materials* **184** (1–3), 555–560.

Xue, Y., Hou, H. & Zhu, S. 2009 Characteristics and mechanisms of phosphate adsorption onto basic oxygen furnace slag. *Journal of Hazardous Materials* **162** (2–3), 973–980.

First received 31 January 2017; accepted in revised form 7 April 2017. Available online 21 April 2017